# ChemComm

Chemical Communications

www.rsc.org/chemcomm

Number 5 | 7 February 2008 | Pages 513–636

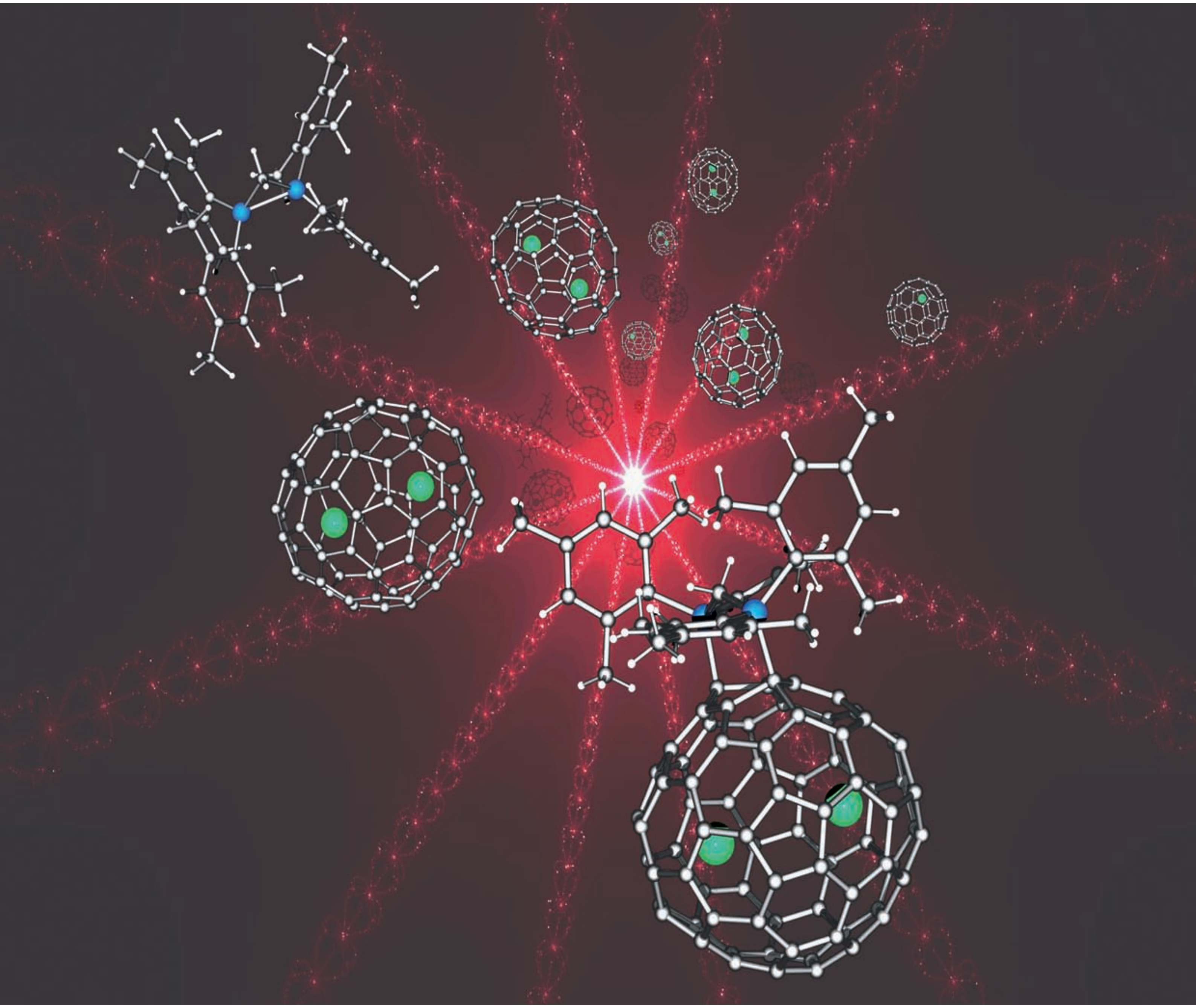

ISSN 1359-7345

RSC Publishing

**COMMUNICATION**

Takeshi Akasaka *et al.*

Location of the metal atoms in $Ce_2@C_{78}$ and its bis-silylated derivative

**FEATURE ARTICLES**

Julio Pérez and Lucia Riera

Organometallic complexes as anion hosts

Catherine J. Murphy *et al.*

Chemical sensing and imaging with metallic nanorods

1359-7345(2008)5;1-2

# Location of the metal atoms in $Ce_2@C_{78}$ and its bis-silylated derivative†

**Michio Yamada,[a] Takatsugu Wakahara,[a] Takahiro Tsuchiya,[a] Yutaka Maeda,[b] Masahiro Kako,[c] Takeshi Akasaka,*[a] Kenji Yoza,[d] Ernst Horn,[e] Naomi Mizorogi[f] and Shigeru Nagase[f]**

***Received (in Cambridge, UK) 15th August 2007, Accepted 15th October 2007***
***First published as an Advance Article on the web 26th October 2007***
**DOI: 10.1039/b712568b**

**Dimetallofullerene $Ce_2@C_{78}$ and its bis-silylated derivative (1) were successfully prepared and fully characterized.**

Endohedral metallofullerenes have received extensive attention for their fascinating structures, properties and chemical reactivities.[1] Especially, considerable interest is now directed toward the dimetallofullerenes such as $La_2@C_{80}$[2] and $Ce_2@C_{80}$[3] because of the three-dimensional random motion of the two metal atoms inside the fullerene cage. However, the dynamic behavior of the metal atoms in other dimetallofullerenes has not been clarified. Recently we reported the first isolation, $^{13}$C NMR characterization, and theoretical studies of a new dimetallofullerene, $La_2@C_{78}$.[4] The $^{13}$C NMR study showed that $La_2@C_{78}$ has a $D_{3h}$–$C_{78}$ cage, because five lines with full intensity and three lines with half intensity were observed. Although there are two $D_{3h}$ IPR cage isomers for $C_{78}$,[5] further structural determination of $La_2@C_{78}$ was not achieved experimentally. Herein we report the synthesis and characterization of $Ce_2@C_{78}$ and its bis-silylated derivative. The location of the metal atoms in $Ce_2@C_{78}$ and the bis-silylated derivative has been investigated by means of spectroscopic and single-crystal X-ray structural analyses.

$Ce_2@C_{78}$ was synthesized and isolated for the first time using a recently developed method.[6] The purity of the isolated $Ce_2@C_{78}$ is >99.9%, as confirmed by mass spectroscopic and HPLC analyses. The visible–NIR spectrum of $Ce_2@C_{78}$ shows characteristic absorptions at 644, 553, and 526 nm, which resembles that of $La_2@C_{78}$. The colors of $Ce_2@C_{78}$ in solution and in the solid state are dark blue and black, respectively. The $^{13}$C NMR spectrum of $Ce_2@C_{78}$ at 298 K shows a total of distinct eight lines derived from the $C_{78}$ cage; five lines (full intensity) at 104.9, 141.8, 152.4, 155.8, and 156.3 ppm and three lines (half intensity) at 131.6, 150.3, and 162.0 ppm. This $^{13}$C NMR pattern is unambiguously attributed to the fact that the carbon cage of $Ce_2@C_{78}$ has $D_{3h}$ symmetry.[5]‡

The bis-silylation of $Ce_2@C_{78}$ was carried out as reported previously for $Ce_2@C_{80}$.[6b] A toluene solution of $Ce_2@C_{78}$ and 1,1,2,2-tetrakis(2,4,6-trimethylphenyl)-1,2-disilirane[7] was heated at 80 °C for 85 h to afford the bis-silylated adduct **1** (Scheme 1), which was readily isolated by the preparative HPLC method. The formation of **1** was confirmed by mass spectroscopic measurement. The colors of **1** in solution and in the solid state are dark yellow and black, respectively. The visible–NIR spectrum of **1** in $CS_2$ shows an absorption maximum at 957 nm, which differs greatly from that of $Ce_2@C_{78}$. This large difference in the absorptions of **1** and $Ce_2@C_{78}$ is ascribed to the fact that the electronic structure is highly changed by the electron donation from the silyl substituent to the $C_{78}$ cage.§

The electronic property of **1** was investigated by cyclic (CV) and differential pulse voltammetry (DPV) measurement. Adduct **1** exhibits one irreversible and one reversible oxidation waves as well as one reversible reduction wave. As compared to $Ce_2@C_{78}$, all the oxidation and reduction potentials of **1** are cathodically shifted to 290 mV. This is because the $C_{78}$ cage is negatively charged to a considerable extent by silylation. Adduct **1** is stable at the first oxidation potential, though the quantitative retro-cycloaddition takes place at the second oxidation potential. In the case of the bis-silylated $M_2@C_{80}$ (M = La[2e] and Ce[3b]), however, the first oxidation potentials are irreversible and the retro-silylation takes place.

The molecular structure of **1** was fully determined by X-ray crystallographic analysis,¶ and its ORTEP drawing is shown in Fig. 1. The two Ce atoms are disordered over two locations with occupancies 0.958/0.042. It is obvious from Fig. 1 that **1** results from the 1,4-addition (positions D and D′ in Fig. 2c) of the disilirane to $Ce_2@C_{78}$ having $D_{3h}$ (78 : 5) cage and the two encapsulated Ce atoms are located at two positions directed toward the hexagonal ring at the $C_3$ axis of the ellipsoidal $C_{78}$ cage, reflecting that these positions are energetically the most stable. Recently the X-ray crystallographic analysis of a cocrystal of $Sc_3N@C_{78}$ and Co(oep) (oep = octaethylporphyrin) has been reported, which shows that the $Sc_3N$ cluster is located near the mirror plane perpendicular to the $C_3$ axis of the $C_{78}$ cage.[8] Two regioisomers of pyrrolidino derivatives of $Sc_3N@C_{78}$ have also been reported, in which the addition sites correspond to B–G and E–F bonds in Fig. 2c.[9] The Ce–Ce distance of 4.036(1) Å in **1** for the major Ce components is considerably longer than that of

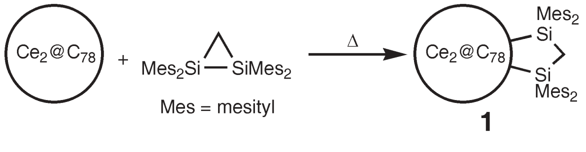

**Scheme 1** Synthesis of the bis-silylated derivative of $Ce_2@C_{78}$.

---

[a] *Center for Tsukuba Advanced Research Alliance, University of Tsukuba, Tsukuba, Ibaraki 305-8577, Japan. E-mail: akasaka@tara.tsukuba.ac.jp; Fax: (+81) 298 53 6409; Tel: (+81) 298 53 6409*
[b] *Department of Chemistry, Tokyo Gakugei University, Koganei, Tokyo 184-8501, Japan*
[c] *Department of Applied Physics and Chemistry, The University of Electro-communications, Chofu, Tokyo 182-8585, Japan*
[d] *Bruker AXS K. K., Yokohama, Kanagawa 221-0022, Japan. E-mail: kenji.yoza@bruker-axs.jp*
[e] *Department of Chemistry, Rikkyo University, Tokyo 171-8501, Japan*
[f] *Department of Theoretical and Computational Molecular Science, Institute for Molecular Science, Okazaki, Aichi 444-8585, Japan. E-mail: nagase@ims.ac.jp*

† Electronic supplementary information (ESI) available: Fig. S1–S21 and Tables S1–S2. See DOI: 10.1039/b712568b

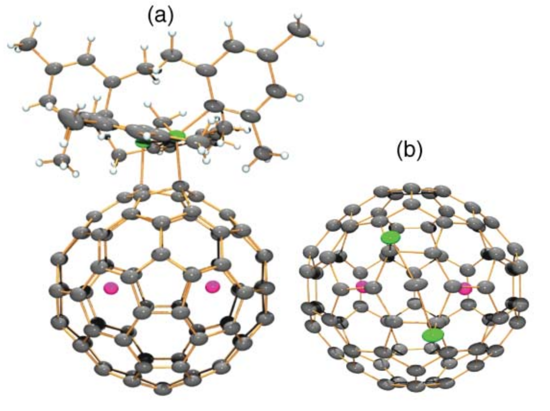

**Fig. 1** (a) Side view and (b) top view of the ORTEP drawings of **1** at 130 K. Thermal ellipsoids are shown at 30% probability level. The $CS_2$ molecules are omitted for clarity. Only one Ce site with the highest occupancy (0.958) is shown. The mesityl groups and hydrogen atoms are also omitted for clarity in (b).

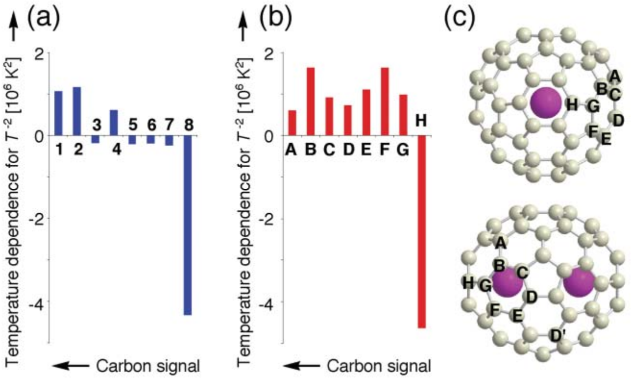

**Fig. 2** (a) The temperature dependence for $T^{-2}$ of the carbon signals of $Ce_2@C_{78}$. Carbon signals line in order of chemical shifts at 283 K. (b) Calculated values of the temperature dependence for $T^{-2}$ of the carbon signals of $Ce_2@C_{78}$. (c) Two views of the optimized structure of $La_2@C_{78}$ which was used for the calculation.

3.829 Å in the bis-silylated $Ce_2@C_{80}$.[6b] The minor Ce–Ce distance is 4.09(3) Å. However, the average distance of 2.510 Å between the Ce atoms and the nearest carbon atoms in **1** differs little from that of 2.521 Å in the bis-silylated $Ce_2@C_{80}$.[6b] The considerably long Ce–Ce distance in **1** is due to the electrostatic repulsion between the two positively charged Ce atoms at the $C_3$ axis of the ellipsoidal $C_{78}$ cage, where the repulsion is minimized. It is also to be noted that the intermolecular separation of 3.06 Å between C34 and C55 of the cage generates a chain of fullerene molecules along the *a*-axis (see Figures S20 and S21).

To clarify the dynamic behavior of the encapsulated Ce atoms, paramagnetic $^{13}C$ NMR spectral analyses[10] were carried out for $Ce_2@C_{78}$ and **1**. All the carbon chemical shifts show considerable temperature dependence originating from the f electron spins remaining on the Ce atoms in $Ce_2@C_{78}$ and **1**. For $Ce_2@C_{78}$, one carbon signal (number 8, see Figure S4) with full intensity is highly shifted to upfield region by decreasing temperatures from 303 to 283 K among the eight signals as shown in Fig. 2a. For the chemical shifts of cerium metallofullerenes, we have recently revealed that the pseudocontact shift ($\delta_{pc}$) proportional to $T^{-2}$ makes a much larger contribution than the Fermi contact interaction shift ($\delta_{fc}$) proportional to $T^{-1}$.[10] The $\delta_{pc}$ value of the temperature dependence for $T^{-2}$ is $-4.3 \times 10^6$ K$^2$, which is obtained by the line-fitting plot of chemical shifts *vs.* $T^{-2}$ (Figure S7). This value is in good agreement with the calculated value of the carbon marked as H (Fig. 2b) where the optimized structure of $La_2@C_{78}$[4] was used for the calculation (Fig. 2c). In addition, the range of the absolute values of the temperature dependence for the other carbon signals is also almost equal to that of the calculated values, though some signals show the opposite signs. This result indicates that the metal position in $Ce_2@C_{78}$ is similar to that in the optimized structure of $La_2@C_{78}$.

On the other hand, the temperature dependence for $T^{-2}$ of the two signals of $Ce_2@C_{80}$ shows much smaller values such as $0.2 \times 10^6$ and $-0.8 \times 10^6$ K$^{2}$[6b] because of the three-dimensional random motion. Therefore, the Ce atoms in $Ce_2@C_{78}$ are localized on the $C_3$ axis of the ellipsoidal $C_{78}$ cage. Some deviations may result from the point charge model for the Ce atom since the Ce atom can oscillate around the energy minimum. For **1**, a total of 58 signals involving 39 signals for the $C_{78}$ skeleton was observed and characterized. As shown in Fig. 3, these carbon signals show a large temperature dependence, as compared with the $Ce_2@C_{78}$ case. This indicates that the two Ce atoms are more tightly localized in **1** than in $Ce_2@C_{78}$.

In conclusion, a new dimetallofullerene, $Ce_2@C_{78}$, and its bis-silylated derivative (**1**) were successfully prepared and fully characterized. The X-ray crystallographic analysis clearly confirms that **1** results from the regioselective 1,4-addition of disilirane to $Ce_2@C_{78}$ having $D_{3h}$ (78 : 5) cage and two Ce atoms stand still by facing toward the hexagonal rings at the equator in **1**. The paramagnetic $^{13}C$ NMR shift spectral analyses reveal that the encapsulated Ce atoms are localized on the $C_3$ axis of the $C_{78}$ cage in $Ce_2@C_{78}$ and more tightly localized in **1**. As shown in this work, chemical derivatization of dimetallofullerenes is expected to be of great help in designing novel molecular devices with new electronic or magnetic properties.

We thank H. Sawa for his experimental help at the Photon Factory. This work was supported in part by a Grant-in-Aid, the 21st Century COE Program, Nanotechnology Support Project, The Next Generation Super Computing Project (Nanoscience Project), and Scientific Research on Priority Area from the Ministry of Education, Culture, Sports, Science, and Technology

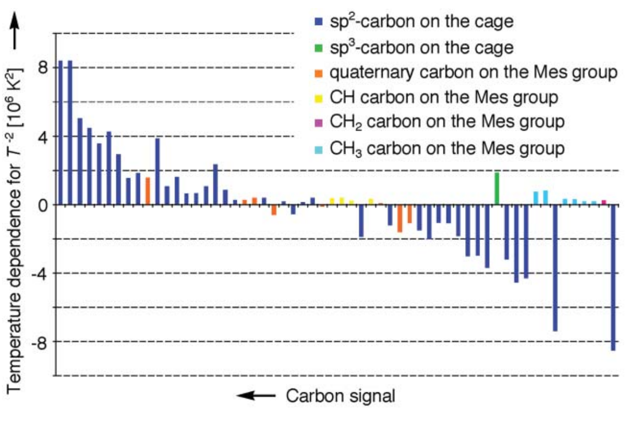

**Fig. 3** The temperature dependence for $T^{-2}$ of the carbon signals of **1**. Carbon signals line in order of chemical shifts at 284 K.

of Japan, and a grant from the Kurata Memorial Hitachi Science and Technology Foundation.

## Notes and references

‡ *Preparation and Purification* of $Ce_2@C_{78}$: The soot containing cerium metallofullerenes was prepared according to the reported procedure[6] using a composite anode which contains graphite and cerium oxide with the atomic ration of Ce to C equal to 2.0%. The composite rod was subjected to an arc discharge as an anode under a 150 Torr He pressure. The raw soot containing cerium metallofullerenes was collected and extracted with *N*,*N*-dimethylformamide (DMF) solvent for 15 h. The soluble fraction was injected into the HPLC; a Buckyprep column (20 mm × 250 mm i.d.; Cosmosil, Nacalai Tesque, Inc.) was used to give pure $Ce_2@C_{78}$.

Spectral data for $Ce_2@C_{78}$: $^{13}$C NMR (125 MHz, $CS_2$ (acetone-$d_6$ in capillary as lock solvent), 293 K) $\delta$ (ppm) 162.4 (6C), 156.8 (12C), 155.7 (12C), 152.7 (12C), 150.3 (6C), 141.8 (12C), 131.6 (6C), 103.2 (12C). Vis–NIR ($CS_2$) $\lambda_{max}$ ($\varepsilon$ [dm$^3$ mol$^{-1}$ cm$^{-1}$]) 644 (6000), 553 (3700), 526 (3700) nm; MALDI-TOF MS *m*/*z* 1216 ($M^-$).

§ *Synthesis* of the adduct **1**: A toluene solution of 20 ml containing $Ce_2@C_{78}$ (2.0 mg, $8.2 \times 10^{-5}$ M) was heated at 80 °C for 85 h with 30 equiv. of 1,1,2,2-tetrakis(2,4,6-trimethylphenyl)-1,2-disilirane[7] under argon atmosphere to achieve the adduct **1**. Adduct **1** can be readily isolated by the preparative HPLC using a Buckyprep column (20 mm × 250 mm i.d.; Cosmosil, Nacalai Tesque, Inc.). Toluene was distilled over benzophenone sodium ketyl under argon atmosphere prior to use. 1,2-Dichlorobenzene (ODCB) was distilled over $P_2O_5$ under vacuum prior to use. $CS_2$ was distilled over $P_2O_5$ under argon atmosphere prior to use. HPLC isolation was performed on a LC-908 (Japan Analytical Industry Co., Ltd.) monitored by UV absorption at 330 nm. Toluene was used as the eluent. Mass spectrometry was performed on a Bruker BIFLEX III with 1,1,4,4-tetraphenyl-1,3-butadiene as matrix. The vis–NIR absorption spectra were measured in $CS_2$ solution by using a SHIMADZU UV-3150 spectrophotometer. Cyclic voltammograms (CV) and differential pulse voltammograms (DPV) were recorded on a BAS CV50W electrochemical analyzer. Platinum wires were used as the working electrode and the counter electrode, respectively. The reference electrode was a saturated calomel reference electrode (SCE) filled with 0.1 M ($n$-Bu)$_4$NPF$_6$ in ODCB. All potentials are referenced to the ferrocene/ferrocenium couple (Fc/Fc$^+$) as the standard. CV: scan rate, 20 mV s$^{-1}$. DPV: Pulse amplitude, 50 mV; pulse width, 50 ms; pulse period, 200 ms; scan rate, 20 mV s$^{-1}$. NMR spectra were obtained with Bruker AVANCE-300, and AVANCE-500 with a CryoProbe system. The $^1$H chemical shifts were calibrated with dichloromethane-$d_2$ as an internal reference ($\delta$ 5.23). $^{13}$C chemical shifts were calibrated with $CS_2$ as an internal reference ($\delta$ 195.0).

Spectral data for **1**: $^1$H NMR (300 MHz, $CS_2/CD_2Cl_2$ = 3/1), 288 K) $\delta$ 10.03 (s, 6H), 9.98 (s, 2H), 9.86 (s, 2H), 9.24 (s, 2H), 8.40 (s, 6H), 8.20 (s, 2H), 8.09 (s, 2H), 5.67 (s, 6H), 4.77 (s, 6H), 3.27 (s, 6H), 3.27 (s, 6H) ppm; $^{13}$C NMR (125 MHz, $CS_2/CD_2Cl_2$ = 3/1), 293 K) $\delta$ 315.2 (2C), 259.2 (2C), 222.4 (2C), 211.9 (2C), 206.3 (2C), 184.6 (2C), 178.7 (2C), 173.3 (2C), 171.8 (2C), 168.6 (2C), 168.6 (2C), 167.0 (2C), 158.8 (2C), 154.2 (2C), 152.5 (2C), 151.7 (2C), 152.4 (2C), 151.0 (2C), 150.7 (2C), 148.1 (2C), 147.5 (2C), 146.8 (2C), 144.3 (2C), 143.7 (2C), 143.1 (2C), 140.5 (2C), 140.1 (2C), 138.3 (2C), 137.6 (2C), 136.3 (2C), 137.4 (2C), 135.3 (2C), 135.2 (2C), 134.5 (2C), 133.9 (2C), 133.0 (2C), 128.8 (2C), 128.5 (2C), 125.6 (2C), 125.0 (2C), 115.4 (2C), 101.9 (2C), 100.0 (2C), 99.6 (2C), 91.2 (2C), 94.7 (2C), 79.2 (2C), 64.5 (2C), 41.4 (2C), 41.0 (2C), 38.1 (2C), 32.2 (2C), 29.8 (2C), 25.3 (2C), 25.2 (2C), 19.9 (2C), 13.9 (1C) ppm. Another peak was overlapped with the signal of $CS_2$. Vis–NIR ($CS_2$) $\lambda_{max}$ 957 nm; MALDI-TOF MS *m*/*z* 1762 ($M^-$), 1216 ($M^- - [(Mes_2Si)_2CH_2]$).

¶ Black crystals of **1** were obtained by evaporating slowly a solution of **1** in $CS_2$ and hexane. Single-crystal X-ray diffraction data were collected on a beamline BL-1B of the Photon Factory (KEK, Japan) at 130, 200, and 270 K. The crystal data for $\mathbf{1}\cdot 2.5(CS_2)$ at 130 K are as follows: $C_{117.5}H_{46}Ce_2S_5Si_2$, fw = 1954.26, orthorhombic, space group $P2_12_12_1$, $a$ = 11.300(2) Å, $b$ = 23.437(4) Å, $c$ = 27.993(6) Å, $\alpha = \beta = \gamma$ = 90.00°, $V$ = 7414(2) Å$^3$, $Z$ = 4, $D_c$ = 1.751 Mg m$^{-3}$, $\mu$ = 1.449 mm$^{-3}$, $T$ = 130 K, crystal size 0.15 × 0.15 × 0.01 mm. 34138 reflections, 10295 unique reflections; 8808 with $I > 2\sigma(I)$; $R_1$ = 0.0491 [$I > 2\sigma(I)$], $wR_2$ = 0.1445 (all data), GOF (on $F^2$) = 1.035. The maximum residual electron density is equal to 1.182 e Å$^{-3}$. CCDC 656005, 661490 and 661491. For crystallographic data in CIF or other electronic format see DOI: 10.1039/b712568b

1 For a recent review, see: *Endofullerenes: A New Family of Carbon Clusters*, ed. T. Akasaka and S. Nagase, Kluwer Academic Publishers, Dordrecht, 2002.

2 (*a*) K. Kobayashi, S. Nagase and T. Akasaka, *Chem. Phys. Lett.*, 1996, **261**, 502–506; (*b*) T. Akasaka, S. Nagase, K. Kobayashi, M. Waelchli, K. Yamamoto, H. Funasaka, M. Kako, T. Hoshino and T. Erata, *Angew. Chem.*, 1997, **109**, 1716–1719, (*Angew. Chem., Int. Ed. Engl.*, 1997, **36**, 1643–1645); (*c*) E. Nishibori, M. Takata, M. Sakata, A. Taninaka and H. Shinohara, *Angew. Chem.*, 2001, **113**, 3086–3087, (*Angew. Chem., Int. Ed.*, 2001, **40**, 2998–2999); (*d*) H. Shimotani, T. Ito, Y. Iwasa, A. Taninaka, H. Shinohara, E. Nishibori, M. Takata and M. Sakata, *J. Am. Chem. Soc.*, 2004, **126**, 364–369; (*e*) T. Wakahara, M. Yamada, S. Takahashi, T. Nakahodo, T. Tsuchiya, Y. Maeda, T. Akasaka, M. Kako, K. Yoza, E. Horn, N. Mizorogi and S. Nagase, *Chem. Commun.*, 2007, 2680–2682.

3 (*a*) J. Ding and S. Yang, *Angew. Chem.*, 1996, **108**, 2369–2371, (*Angew. Chem., Int. Ed. Engl.*, 1996, **35**, 2234–2235); (*b*) M. Yamada, T. Nakahodo, T. Wakahara, T. Tsuchiya, Y. Maeda, T. Akasaka, M. Kako, K. Yoza, E. Horn, N. Mizorogi, K. Kobayashi and S. Nagase, *J. Am. Chem. Soc.*, 2005, **127**, 14570–14571.

4 B. Cao, T. Wakahara, T. Tsuchiya, M. Kondo, Y. Maeda, G. M. A. Rahman, T. Akasaka, K. Kobayashi, S. Nagase and K. Yamamoto, *J. Am. Chem. Soc.*, 2004, **126**, 9164–9165.

5 P. W. Fowler and D. E. Manolopoulos, in *An Atlas of Fullerenes,* Clarendon Press, Oxford, 1995, pp 254–255.

6 (*a*) T. Tsuchiya, T. Wakahara, S. Shirakura, Y. Maeda, T. Akasaka, K. Kobayashi, S. Nagase, T. Kato and K. M. Kadish, *Chem. Mater.*, 2004, **16**, 4343–4346; (*b*) M. Yamada, T. Nakahodo, T. Wakahara, T. Tsuchiya, Y. Maeda, T. Akasaka, M. Kako, K. Yoza, E. Horn, N. Mizorogi and S. Nagase, *J. Am. Chem. Soc.*, 2005, **127**, 14570–14571.

7 (*a*) W. Ando, M. Kako, T. Akasaka and S. Nagase, *Organometallics*, 1993, **12**, 1514–1522 and references cited therein; (*b*) W. Ando, M. Kako and T. Akasaka, *J. Am. Chem. Soc.*, 1991, **113**, 6286–6288.

8 M. M. Olmstead, A. de Bettencourt-Dias, J. C. Duchamp, S. Stevenson, D. Marciu, H. C. Dorn and A. L. Balch, *Angew. Chem.*, 2001, **113**, 1263–1265, (*Angew. Chem., Int. Ed.*, 2001, **40**, 1223–1225).

9 T. Cai, L. Xu, H. W. Gibson, H. C. Dorn, C. J. Chancellor, M. M. Olmstead and A. L. Balch, *J. Am. Chem. Soc.*, 2007, **129**, 10795–10800.

10 M. Yamada, T. Wakahara, Y. Lian, T. Tsuchiya, T. Akasaka, M. Waelchli, N. Mizorogi, S. Nagase and K. M. Kadish, *J. Am. Chem. Soc.*, 2006, **128**, 1400–1401.